CHAPTER IV
RESULTS AND DISCUSSION

4.1 Effects of Feed Composition on *m*- and *p*-CNB Crystallization

The starting liquid mixtures at 20.0, 30.0, 50.0, 61.0, 62.9, 70.0, and 80 wt% *m*-CNB were used to study the effects of feed compositions on the *m*- and *p*-CNB crystallization and to construct the binary phase diagram. Seven grams of solid *m*- and *p*-CNB were melted to obtain a homogeneous liquid solution. The liquid mixture was measured for the CNB compositions by using the GC. Then, the liquid mixture in the crystallizer was cooled by the cooling water to a crystallization temperature. All precipitates were collected from the crystallizer, washed, and dissolved with hexane. The dissolved precipitates were measured for the CNB compositions by using the GC. The starting feed composition and the solid composition with different starting liquid mixtures are shown in Tables 4.1. The crystallization of the feed below the eutectic composition (20, 30, 50, 61 wt% *m*-CNB) results in the crystal form. The composition is rich in *p*-CNB. On the contrary, when the feed composition at the eutectic composition (62.9 wt% *m*-CNB) is cooled down to the crystallization temperature at 22 °C, an amorphous solid with the composition close to the feed composition can be observed. Crystallization of the feed above the eutectic composition results in the crystal form, which is the same with that below the eutectic composition but the composition is rich in *m*-CNB. As a whole, the result shows the purity of the precipitate composition is not close to 100 wt%. In the industrial crystallization practice, many bulk-produced chemicals with a purity more than 95 percent are often accepted as justifying the designation "pure". Generally, crystals contain foreign impurities or called "inclusion" (Mullin, 2001). The results conform to the binary phase diagram, as shown in Figure 4.1.

Table 4.1 Composition of *m*- and *p*-CNB in the feeds and solids, and crystallization temperatures

Feed	Feed composition (wt%)		Precipitate composition (wt%)		Crystallization temperature (°C)
	m-CNB	*p*-CNB	*m*-CNB	*p*-CNB	
Below the eutectic	20.09 **[1]**	79.91 **[1]**	1.72 **[1]**	98.28 **[1]**	67.5
	19.36 **[2]**	80.64 **[2]**	1.42 **[2]**	98.58 **[2]**	67.5
	29.68 **[1]**	70.32 **[1]**	1.25 **[1]**	98.75 **[1]**	58.0
	30.09 **[2]**	69.91 **[2]**	1.94 **[2]**	98.06 **[2]**	58.0
	50.40 **[1]**	49.60 **[1]**	4.89 **[1]**	95.11 **[1]**	39.0
	49.68 **[2]**	50.32 **[2]**	2.71 **[2]**	97.29 **[2]**	39.0
	60.74 **[1]**	39.26 **[1]**	5.83 **[1]**	94.17 **[1]**	24.0
	60.72 **[2]**	39.28 **[2]**	5.79 **[2]**	94.21 **[2]**	24.0
The eutectic	62.85 **[1]**	37.15 **[1]**	62.70 **[1]**	37.30 **[1]**	22.0
	62.78 **[2]**	37.22 **[2]**	62.90 **[2]**	37.10 **[2]**	22.0
	62.63 **[3]**	37.37 **[3]**	62.76 **[3]**	37.24 **[3]**	22.0
Above the eutectic	69.99 **[1]**	30.01 **[1]**	98.87 **[1]**	1.13 **[1]**	25.0
	70.04 **[2]**	29.96 **[2]**	98.58 **[2]**	1.42 **[2]**	25.0
	79.45 **[1]**	20.55 **[1]**	98.29 **[1]**	1.71 **[1]**	29.0
	80.02 **[2]**	19.98 **[2]**	98.81 **[2]**	1.19 **[2]**	29.0

Note: [*], * refers to the run number.

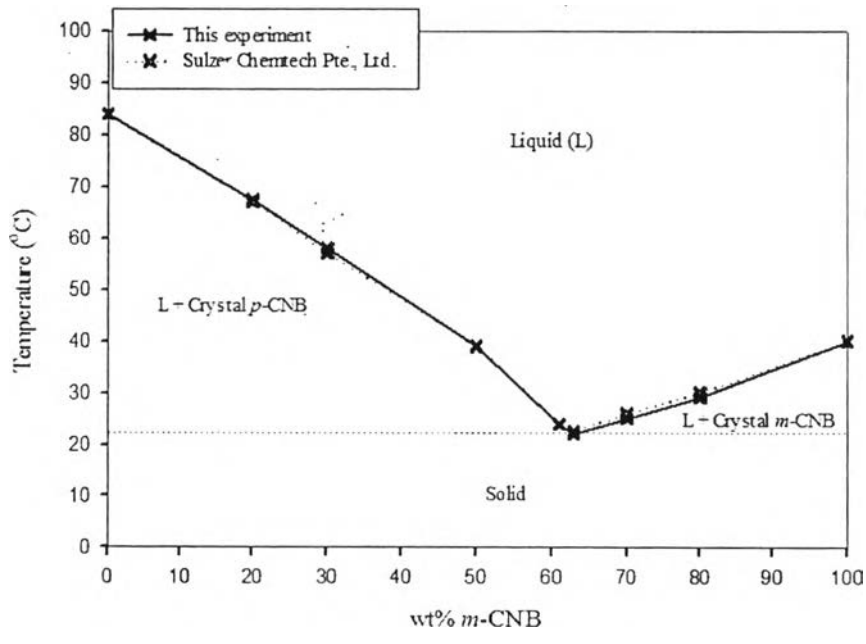

Figure 4.1 Composition of binary phase diagram of *m*- and *p*-CNB between this experiment and Sulzer Chemtech Pte., Ltd.

4.2 Effects of Seeds on the Crystallization

4.2.1 Effects of Seeds on the CNB Feed Solution Compositions

To investigate the effects of various seeds on the feed composition, experiments were carried out with below, at, and above the eutectic composition (61.0, 62.9, and 70 wt% *m*-CNB in the feed, respectively). Below the eutectic composition, 7 grams of 0.61 and 0.39 mass fraction of *m*-CNB and *p*-CNB were melted to obtain a homogeneous liquid mixture. Two types of solid were used as the seed, *m*- and *p*-CNB. After a given time, the mixture compositions after adding a seeds were determined by the GC. The results are shown in Tables 4.2 and 4.3. The feed compositions before and after adding the seeds are almost the same regardless of the particle size and type of the seeds; therefore, it may be concluded that the particle size and type of the seeds do not significantly affect the feed composition.

Table 4.2 *m*- and *p*-CNB composition in the feed with 61.0, 62.9 and 70.0 wt% of *m*-CNB before and after adding size 20/40 mesh of seeds at 30 °C

Seeds	Feed composition before adding seeds (wt%)		Precipitate composition after adding seeds (wt%)	
	m-CNB	*p*-CNB	*m*-CNB	*p*-CNB
m-CNB	60.51	39.49	60.58	39.42
	62.42	37.58	62.15	37.85
	70.12	29.88	70.08	29.92
p-CNB	60.96	39.04	61.43	38.57
	62.22	37.78	62.20	37.80
	69.91	30.09	69.23	30.77

Table 4.3 *m*- and *p*-CNB composition in the feed with 61.0, 62.9 and 65.0 wt% of *m*-CNB before and after adding size 12/14 mesh of seeds at 30 °C

Seeds	Feed composition before adding seeds (wt%)		Precipitate composition after adding seeds (wt%)	
	m-CNB	*p*-CNB	*m*-CNB	*p*-CNB
m-CNB	60.23	39.77	60.79	39.21
	62.48	37.52	62.47	37.53
	64.70	35.30	64.91	35.09
p-CNB	60.35	39.65	60.33	39.67
	62.67	37.33	62.65	37.35
	64.67	35.33	64.74	35.26

4.2.2 Effects of *m*-CNB Seeds on the CNB Solid Composition and Crystallization Temperature

The effects of different *m*-CNB seed sizes on the CNB solid composition and crystallization temperature were investigated. Five grains of the *m*-CNB seeds were added at the center of the CNB mixture in the crystallizer. The mixture was cooled by the cooling water from 30 °C to the crystallization temperature with a 1°C/hr cooling rate. The crystallization temperature; and feed and solid composition are shown in Tables 4.4 and 4.5. The crystallization of the feed with the composition below and above the eutectic composition results in the crystal form regardless of the seed size. Below the eutectic composition, the crystals are rich in *p*-CNB. At the eutectic composition, 65.0 wt% *m*-CNB, the feed can be crystallized at 21.5 °C, with the small particle size of *m*-CNB seeds (20/40 mesh), the amorphous solid is formed. By contrast, with the large particle size (12/14 mesh), at the eutectic composition, the crystallization on the feed composition becomes an amorphous solid at 21.0 °C. Likewise, the feed compositions at 67.5 and 70.0 wt% *m*-CNB (above the eutectic) in the crystallization results in the crystals rich in *m*-CNB. Comparison between the crystallization without and with the *m*-CNB seeds shows that the crystallization temperature in the system without the seeds is 22.0 °C, at the eutectic composition, which is higher than that with the seed about 0.5 and 1.0 °C, for small and large seed sizes, respectively. However, there is no significant change in the solid composition between both cases. The results conform to the binary phase diagram, as shown in Figures 4.2 and 4.3. The eutectic composition is at 65 wt% *m*-CNB for both particle sizes, and the eutectic temperature with the small particle size (20/40 mesh) is about 0.5 °C higher than that large particle size (12/14 mesh) of the same *m*-CNB seed. As a whole, it can be concluded that two different sizes of m-CNB seed hardly affect the temperature at the eutectic composition. Nevertheless, the crystallization temperature of small seed size is slightly higher than that large particle size. It may be because the large seed size exhibits a slow growth rate. Another reason may come from the metastable zone width and interfacial tension. In the crystallization processes, supersaturated solution exhibit a metastable zone. The metastable zone width result from the specific characteristics of nucleation in a supersaturated solution of soluble substances. The metastable zone width is

considered as a characteristic property of crystallization, and depend on temperature, solution, cooling rate and presence of impurity.

Table 4.4 Composition of *m*- and *p*-CNB in the crystals with 5 grains of 20/40 mesh *m*-CNB seed size

Feed	Feed composition (wt%)		Precipitate composition (wt%)		Crystallization temperature (°C)
	m-CNB	*p*-CNB	*m*-CNB	*p*-CNB	
Below the eutectic	60.27 **[1]**	39.73 **[1]**	9.76 **[1]**	90.24 **[1]**	25.0
	60.21 **[2]**	39.79 **[2]**	5.93 **[2]**	94.07 **[2]**	25.0
	60.37 **[3]**	39.63 **[3]**	6.17 **[3]**	93.83 **[3]**	25.0
	62.31 **[1]**	37.69 **[1]**	6.55 **[1]**	93.45 **[1]**	23.0
	62.43 **[2]**	37.57 **[2]**	6.01 **[2]**	93.99 **[2]**	23.0
	62.52 **[3]**	37.48 **[3]**	5.49 **[3]**	94.51 **[3]**	23.0
At the eutectic	64.64 **[1]**	35.36 **[1]**	65.08 **[1]**	34.92 **[1]**	20.5
	64.66 **[2]**	35.34 **[2]**	64.11 **[2]**	35.89 **[2]**	21.5
	64.63 **[3]**	35.37 **[3]**	65.04 **[3]**	34.96 **[3]**	21.5
Above the eutectic	67.99 **[1]**	32.01 **[1]**	92.50 **[1]**	7.50 **[1]**	25.0
	69.18 **[2]**	30.82 **[2]**	99.16 **[2]**	0.84 **[2]**	25.0
	70.03 **[3]**	29.97 **[3]**	97.67 **[3]**	2.33 **[3]**	25.0

Note: [*], * refers to the run number.

Table 4.5 Composition of *m*- and *p*-CNB in the crystals with 5 grains of 12/14 mesh *m*-CNB seed size

Feed	Feed composition (wt%)		Precipitate composition (wt%)		Crystallization temperature (°C)
	m-CNB	*p*-CNB	*m*-CNB	*p*-CNB	
Below the eutectic	60.23 **[1]**	39.77 **[1]**	3.09 **[1]**	96.91 **[1]**	24.5
	60.47 **[2]**	39.53 **[2]**	4.85 **[2]**	95.15 **[2]**	25.0
	60.87 **[3]**	39.13 **[3]**	4.11 **[3]**	95.89 **[3]**	25.0
At the eutectic	64.70 **[1]**	35.30 **[1]**	68.07 **[1]**	31.93 **[1]**	21.0
	64.71 **[2]**	35.29 **[2]**	68.58 **[2]**	31.42 **[2]**	21.0
	64.74 **[3]**	35.26 **[3]**	65.77 **[3]**	34.23 **[3]**	21.0
Above the eutectic	68.92 **[1]**	31.08 **[1]**	93.55 **[1]**	6.45 **[1]**	25.0
	69.81 **[2]**	30.19 **[2]**	97.95 **[2]**	2.05 **[2]**	25.0
	70.12 **[3]**	29.88 **[3]**	95.36 **[3]**	4.64 **[3]**	25.0

Note: [*], * refers to the run number.

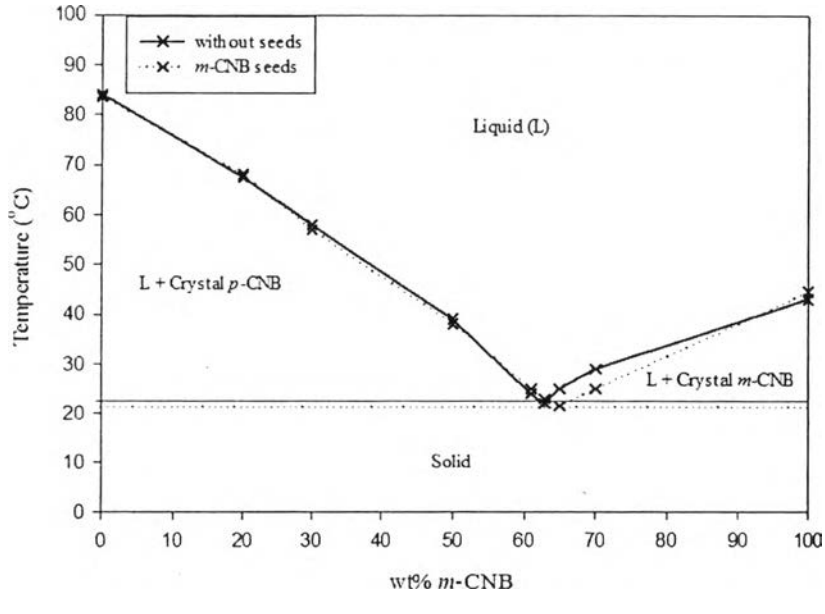

Figure 4.2 Binary phase diagram of *m*- and *p*-CNB with the presence of 20/40 mesh *m*-CNB seed size.

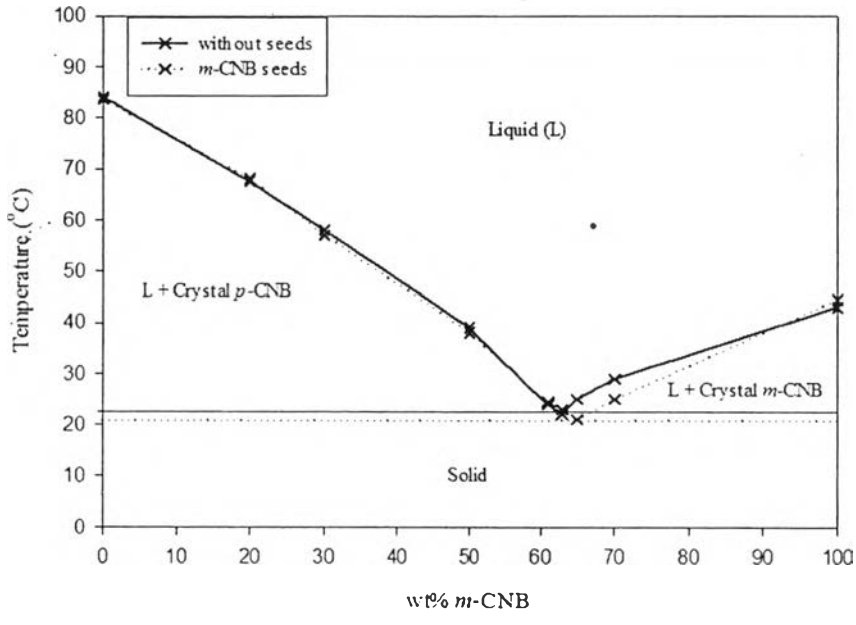

Figure 4.3 Binary phase diagram of *m*- and *p*-CNB with the presence of 12/14 mesh *m*-CNB seed size.

The binary phase diagram of *m*- and *p*-CNB with the presence of different *m*-CNB seed sizes is shown in Figure 4.2. Above the liquidus is homogeneous liquid of *m*-CNB and *p*-CNB. Below the solidus is solid. Below the eutectic composition (61.0 wt% *m*-CNB), where the feed solution is cooled down to the crystallization temperature, the crystal solid of *p*-CNB forms. When the feed solution above the eutectic composition (70.0 wt% m-CNB) is cooled down, the *m*-CNB solid crystal form is obtained. The sectors contain mixtures of crystal *p*-CNB + solution of *m*- and *p*-CNB and crystal *m*-CNB + solution of *m*- and *p*-CNB, respectively. The eutectic composition in this phase diagram is 65.0 wt% *m*-CNB and 35.0 wt% *p*-CNB with the crystallization temperature is 21.5 °C, with the small particle size (20/40 mesh), while the crystallization temperature with the presence of the large particle size (12/14 mesh) the eutectic composition is 21.0 °C.

4.2.3 Effects of *p*-CNB Seeds on the CNB Solid Composition and Crystallization Temperature

Tables 4.6 and 4.7 show the feed composition, solid composition, and crystallization temperature of *m*- and *p*-CNB in the presence of different *p*-CNB seed sizes. Crystallization of the feed with 60.0 - 62.0 wt% *m*-CNB results in the crystals rich in *p*-CNB, while the crystallization of the feed with 70.0 wt% *m*-CNB results in the crystal rich in *m*-CNB. Like the system with the *m*-CNB seeds, the eutectic composition of the system with the small *p*-CNB seed size is now at 65.0 wt% *m*-CNB with 19.0 °C eutectic temperature. On the contrary, with the large size of *p*-CNB seeds, the eutectic temperature is 19.5 °C. Comparison of the solid liquid phase diagram of *m*- and *p*-CNB without and with *p*-CNB seeds are shown in Figures 4.4 and 4.5 for small (20/40 mesh) and large (12/14 mesh) particle size, respectively. It can be concluded that the eutectic composition from the system with the difference particle sizes of *p*-CNB seeds is 65.0 wt% *m*-CNB, which is the same as that with the *m*-CNB seeds. The eutectic temperature of the small particle size (20/40 mesh) is about 0.5 °C lower than that with large particle size of *p*-CNB seeds.

It can be summarized that the *p*-CNB seed is added at the eutectic composition, the crystallization temperature at the eutectic composition of the small seed size is slightly lower than that of the large seed size, which is different from adding *m*-CNB seed as mentioned before. It is interesting to note that the alteration of *p*-CNB seed may depend on specific characteristic of substance. Since, in this study, the crystallization temperature is very important, the seed size must be carefully observed.

Table 4.6 Composition of *m*- and *p*-CNB in the crystals with 5 grains of 20/40 mesh *p*-CNB seed size

Feed	Feed composition (wt%)		Precipitate composition (wt%)		Crystallization temperature (°C)
	m-CNB	*p*-CNB	*m*-CNB	*p*-CNB	
Below the eutectic	60.79 **[1]**	39.21 **[1]**	3.73 **[1]**	96.27 **[1]**	25.0
	60.96 **[2]**	39.04 **[2]**	5.95 **[2]**	94.05 **[2]**	25.0
	61.88 **[3]**	38.12 **[3]**	4.95 **[3]**	95.05 **[3]**	25.0
	62.11 **[1]**	37.89 **[1]**	5.86 **[1]**	94.14 **[1]**	23.0
	62.23 **[2]**	37.77 **[2]**	6.17 **[2]**	93.83 **[2]**	23.0
	62.54 **[3]**	37.46 **[3]**	4.22 **[3]**	95.78 **[3]**	23.0
At the eutectic	64.93 **[1]**	35.07 **[1]**	64.59 **[1]**	35.41 **[1]**	19.0
	64.55 **[2]**	35.45 **[2]**	65.93 **[2]**	34.07 **[2]**	19.0
	64.81 **[3]**	35.19 **[3]**	65. 03 **[3]**	34.97 **[3]**	19.0
Above the eutectic	69.19 **[1]**	30.81 **[1]**	87.77 **[1]**	12.23 **[1]**	23.0
	68.98 **[2]**	31.02 **[2]**	84.18 **[2]**	15.82 [2]	23.0
	69.07 **[3]**	30.93 **[3]**	89.03 **[3]**	10.97 **[3]**	23.0

Note: [*], * refers to the run number.

Table 4.7 Composition of *m*- and *p*-CNB in the crystals with 5 grains of 12/14 mesh *p*-CNB seed size

Feed	Feed composition (wt%)		Precipitate composition (wt%)		Crystallization temperature (°C)
	m-CNB	*p*-CNB	*m*-CNB	*p*-CNB	
Below the eutectic	60.35 **[1]**	39.65 **[1]**	7.06 **[1]**	92.94 **[1]**	25.0
	60.08 **[2]**	39.92 **[2]**	4.51 **[2]**	95.49 **[2]**	25.0
	61.18 **[1]**	38.82 **[1]**	5.49 **[1]**	94.51 **[1]**	24.0
	61.11 **[2]**	38.89 **[2]**	4.75 **[2]**	95.25 **[2]**	24.0
	61.36**[3]**	38.64 **[3]**	4.42 **[3]**	95.58 **[3]**	24.0
At the eutectic	64.67 **[1]**	35.33 **[1]**	65.18 **[1]**	34.82 **[1]**	19.5
	64.37 **[2]**	35.63 **[2]**	64.58 **[2]**	35.42 **[2]**	19.5
	64.59 **[3]**	35.41 **[3]**	64.83 **[3]**	35.17 **[3]**	19.5
Above the eutectic	69.69 **[1]**	30.31 **[1]**	88.91 **[1]**	11.09 **[1]**	23.0
	69.44 **[2]**	30.56 **[2]**	79.54 **[2]**	20.46 **[2]**	23.0
	69.58 **[3]**	30.42 **[3]**	87.26 **[3]**	12.74 **[3]**	23.0

Note: [*], * refers to the run number.

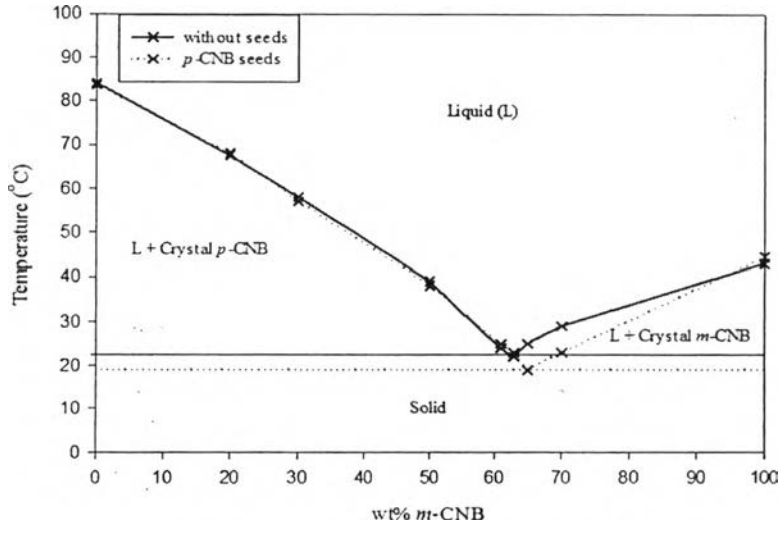

Figure 4.4 Binary phase diagram of *m*- and *p*-CNB with the presence of 20/40 mesh *p*-CNB seed size.

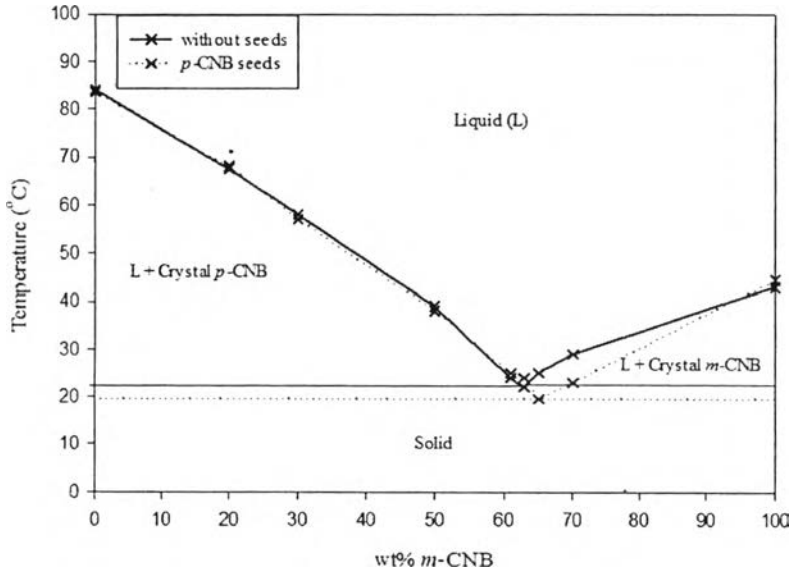

Figure 4.5 Binary phase diagram of *m*- and *p*-CNB with the presence of 12/14 mesh *p*-CNB seed size.

4.2.4 Effects of KY zeolite on the CNB Solid Composition and Crystallization Temperature

The effect of KY zeolite on the CNB precipitate composition and crystallization temperature were investigated. Five grains of the KY zeolite were added at the center of the CNB mixture in the crystallizer. The feed composition, solid composition and crystallization temperature are shown in Tables 4.8 and 4.9. With the presence of the difference particle size of KY zeolite, the crystallization of the feed with 61 wt% *m*-CNB and 70 wt% *m*-CNB results in the crystal form. The crystal obtained from the crystallization of the feed with below the eutectic, 61 wt% *m*-CNB are rich in *p*-CNB, while those from 70 wt% *m*-CNB (above the eutectic) is rich in *m*-CNB. The eutectic composition of the system with small particle size (20/40 mesh) of KY zeolite is now at 65.5 wt% *m*-CNB with the eutectic temperature at 18.5 °C. On the contrary, the eutectic composition of KY zeolite with the large particle size (12/14 mesh) is 65.0 wt% *m*-CNB, and the eutectic temperature is 18.5 °C.

Figures 4.6 and 4.7 show the comparison between the solid liquid phase diagrams of *m*- and *p*-CNB without and with the KY zeolite. The

crystallization on the feed at 62.9 wt% *m*-CNB, which is the eutectic composition of the *m*- and *p*-CNB mixture, results in an amorphous solid form. The crystallization with the addition of KY zeolite clearly results in the crystal formation, not the amorphous solid as in the case when there is no zeolite. The eutectic temperature is lower than that without the KY zeolite, lower about 3.5 °C. Furthermore, the eutectic composition is shifted from 62.9 to 65.5 and 65.0 wt% *m*-CNB in the presence of 20/40 and 12/14 mesh KY zeolite sizes, respectively. In addition, the precipitates from the crystallization on the feed above the eutectic are shifted from being rich in *m*-CNB to rich in *p*-CNB composition, which was also reported by Jukkaew (2013).

Table 4.8 Composition of *m*- and *p*-CNB in the crystals with 5 grains of 20/40 mesh KY zeolite size

Feed	Feed composition (wt%)		Precipitate composition (wt%)		Crystallization temperature (°C)
	m-CNB	*p*-CNB	*m*-CNB	*p*-CNB	
Below the eutectic	61.05 **[1]**	38.95 [1]	2.14 **[1]**	97.86 **[1]**	24.0
	61.07 **[2]**	38.93 **[2]**	3.27 **[2]**	96.23 **[2]**	24.0
At the eutectic	65.55 **[1]**	34.45 **[1]**	65.49 **[1]**	34.51 **[1]**	18.5
	65.25 **[2]**	34.75 **[2]**	65.33 **[2]**	34.67 **[2]**	18.5
	65.11 **[3]**	34.89 **[3]**	65.07 **[3]**	34.93 **[3]**	18.5
Above the eutectic	70.03 **[1]**	29.97 **[1]**	4.11 **[1]**	95.89 **[1]**	20.5
	70.12 **[2]**	29.88 **[2]**	4.69 **[2]**	95.31 **[2]**	20.5
	70.32 **[3]**	29.68 **[3]**	3.89 **[3]**	96.11 **[3]**	20.5

Note: [*], * refers to the run number.

Table 4.9 Composition of *m*- and *p*-CNB in the crystals with 5 grains of 12/14 mesh KY zeolite size

Feed	Feed composition (wt%)		Precipitate composition (wt%)		Crystallization temperature (°C)
	m-CNB	*p*-CNB	*m*-CNB	*p*-CNB	
Below the eutectic	60.31 **[1]**	39.69 **[1]**	6.29 **[1]**	93.71 **[1]**	24.0
	60.26 **[2]**	39.74 **[2]**	6.03 **[2]**	93.97 **[2]**	24.0
At the eutectic	64.73 **[1]**	35.27 **[1]**	65.27 **[1]**	34.73 **[1]**	18.5
	64.51 **[2]**	35.49 **[2]**	65.21 **[2]**	34.79 **[2]**	18.5
	64.82 **[3]**	35.18 **[3]**	65.09 **[3]**	34.91 **[3]**	18.5
Above the eutectic	69.50 **[1]**	30.50 **[1]**	5.25 **[1]**	94.75 **[1]**	20.5
	71.09 **[2]**	28.91 **[2]**	4.78 **[2]**	95.22 **[2]**	20.5
	75.86 **[3]**	24.14 **[3]**	5.19 **[3]**	94.81 **[3]**	21.0

Note: [*], * refers to the run number.

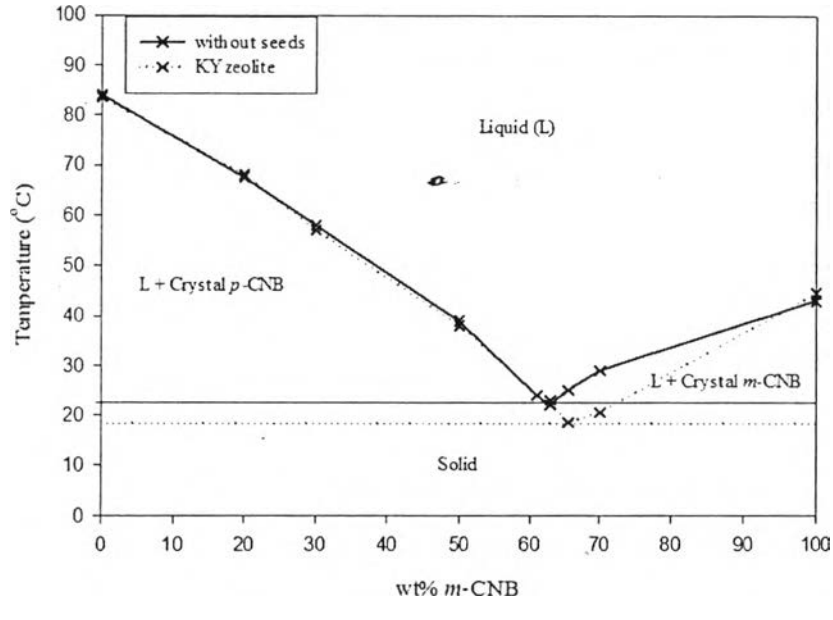

Figure 4.6 Binary phase diagram of *m*- and *p*-CNB with the presence of 20/40 mesh the KY zeolite size.

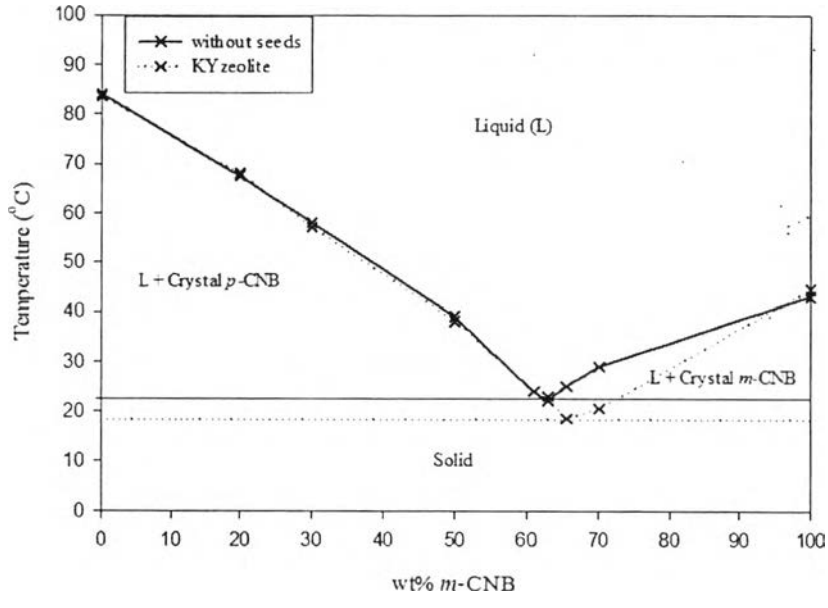

Figure 4.7 Binary phase diagram of *m*- and *p*-CNB with the presence of 12/14 mesh the KY zeolite size.

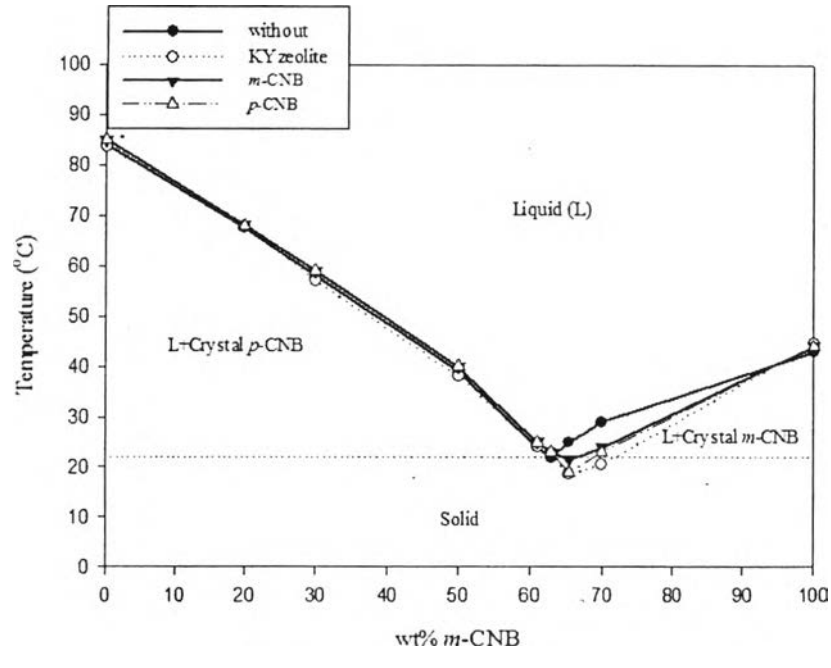

Figure 4.8 Binary phase diagram of *m*- and *p*-CNB with the presence of 20/40 mesh *m*-CNB seed, *p*-CNB seed, and KY zeolite size.

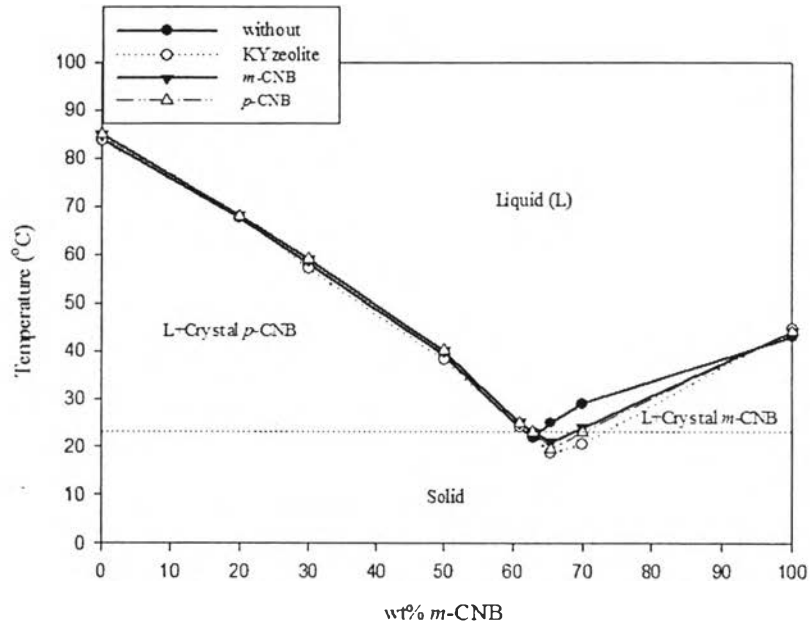

Figure 4.9 Binary phase diagram of *m*- and *p*-CNB with the presence of 12/14 mesh *m*-CNB seed, *p*-CNB seed, and KY zeolite size.

All things considered, seeding has an impact on crystallization mechanism such as secondary nucleation and agglomeration and on the purity of the final product. The main characteristic of particle are crystal size and crystal size distribution (Funakoshi *et al.* 2001). Therefore, the seed crystal surface or seed size is an important factor in crystal growth. As the result from this experiment, from Figures 4.8 and 4.9, the small seed size (20/40 mesh) and the large seed size (12/14 mesh) can be observed. Adding two seed types (*m*- and *p*-CNB seeds) into the CNB liquid mixture at the eutectic composition, the crystallization temperature is higher than that adding KY zeolite. It is obvious that the seeds can induce nucleation step faster than KY zeolite. Indeed, the results from this experiment show that, regardless of particle size of seeding, the two seeds (*m*- and *p*-CNB seeds) behave similarly to the feed solution or the same substances of product. In the nucleation step, the presence of seeds may induce primary nucleation in the heterogeneous nucleation at higher supersaturation or supercooling condition than that the presence of zeolite because seeding, which may reduce energy of nucleation formation in crystallization step.

4.3 Roles of Different Seed Sizes on the *m*- and *p*-CNB Crystallization

Comparison the effect of two types of seeds with different particle size on the phase diagram of *m*- and *p*-CNB is shown in Figures 4.8 and 4.9. Adding *m*- and *p*-CNB as the seeds into the CNB mixture results in the decrease in the crystallization temperature and increase in the eutectic composition on the binary phase diagram. The behavior is the same as when the KY zeolite is added. Results from this experiment show that, regardless of *m*-CNB selectivity or even type of solid material in the CNB mixture, the presence of the seeds or solid material has more or less the same behavior. Effects of the *m*- and *p*- CNB seed may only play a role as seeding rather than having any role on the adsorption.

The reasons why the presence of seeds at the eutectic composition in the feed can shift from amorphous solid into rich in *p*-CNB crystals form may come from the metastable zone width, interfacial tension, and structure change of solution. As a result of the presence of seeds in the CNB mixture, the crystallization temperature is lower than that in the system without any seed. The metastable zone width is explained by the solubility-supersolubility diagram, as shown in Figure 4.10, for interfacial tension associates with the overall free energy change under heterogeneous conditions $\Delta G'_{crit}$ and the overall free energy change under homogeneous nucleation ΔG_{crit}.

The relationship between supersaturation and spontaneous crystallization led to a diagrammatic representation of the metastable zone on a solubility-supersolubility diagram, as shown in Figure 4.10. The lower continuous solubility curve can be located with precision. The upper broken supersolubility curve, which represents temperatures and concentrations, at which uncontrolled spontaneous crystallization occurs, is not as well defined as that of the solubility curve. Its position in the diagram is considerably affected by, amongst other things, the rate at which supersaturation is generated, the intensity of agitation, the presence of trace impurities and the thermal history of the solution. The diagram is divided into three zone (Mullin, 2001):

1. The stable (unsaturated) zone, where crystallization is impossible.

2. The metastable (supersaturated) zone, between the solubility and supersolubility curve, where spontaneous crystallization is impossible. However, if a crystal seed were placed in such a metastable solution, growth would occur on it.
3. The unstable or labile (supersaturated) zone, where spontaneous crystallization is possible, but not inevitable.

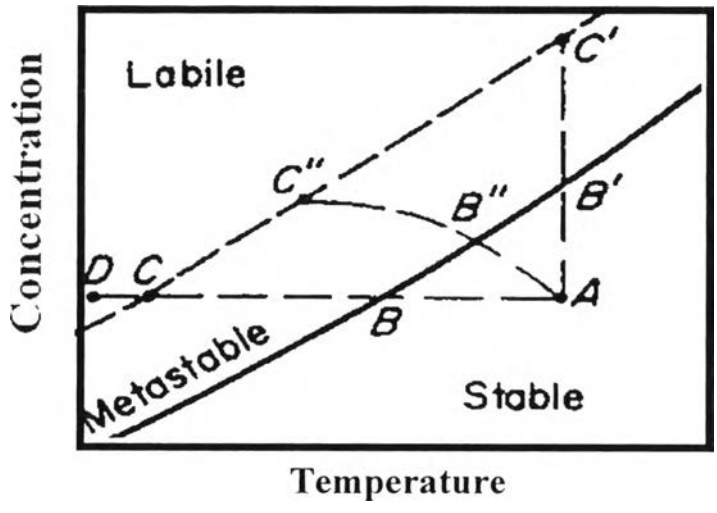

Figure 4.10 Solubility-supersolubility diagram (Mullin, 2001).

If a solution represented by point *A* in Figure 4.10 is cooled without loss of solvent (line *ABC*), spontaneous crystallization cannot occur until conditions represented by point *C* are reached. At this point, crystallization may be spontaneous or it may be induced by seeding, agitation or mechanical shock. Further cooling to some point *D* may be necessary before crystallization can be induced (Mullin, 2001). The position in the diagram is considerably effected by the presence of trace impurities (Mullin, 2001) so that the presence of seeds in the CNB mixture may change the position in the diagram as well.

The maximum allowable supersaturation, Δc_{max}, may be expressed in terms of the maximum allowable undercooling, $\Delta\theta_{max}$:

$$\Delta c_{max} = \left(\frac{dc^*}{d\theta}\right)\Delta\theta_{max} \tag{4.1}$$

As the presence of a suitable foreign body or 'sympathic' surface can induce nucleation at degree of supercooling lower than those required for spontaneous nucleation (Mullin, 2001). This sentence is consistent with crystallization temperature in the presence of seeds, which is lower than in the absence of *m*- and *p*-CNB seeds. When the degree of supercooling decreases, $\Delta\theta_{max}$ and Δc_{max} increase according to the relationship between $\Delta\theta_{max}$ and Δc_{max} in Equation (4.1). Increasing $\Delta\theta_{max}$ and Δc_{max} results in a broader metastable zone width.

The overall free energy change associated with the formation of a critical nucleus under heterogeneous conditions, $\Delta G'_{crit}$, must be less than the corresponding free energy change, ΔG_{crit}, associated with homogeneous nucleation, i.e. (Mullin, 2001).

$$\Delta G'_{crit} = \phi \Delta G_{crit} \tag{4.2}$$

where the factor ϕ is less than unity.

The interfacial tension, γ, is one of the important factors controlling the nucleation process. Figure 4.11 shows an interfacial energy diagram for three phases in contact; in this case, however, the three phases are not the more familiar solid, liquid, and gas, but two solids and a liquid. The three interfacial tensions are denoted by γ_{cl} (between the solid crystalline phase, c, and the liquid l), γ_{sl} (between another foreign solid surface, s, and the liquid) and γ_{cs} (between the solid crystalline phase and foreign solid surface) (Mullin, 2001). Resolving these forces in a horizontal direction

$$\gamma_{sl} = \gamma_{cs} + \gamma_{cl}\cos\theta \tag{4.3}$$

or

$$\cos\theta = \frac{\gamma_{sl} - \gamma_{cs}}{\gamma_{cl}} \tag{4.4}$$

The angle, θ, of contact between the crystalline deposit and foreign solid surface, corresponds to the angle of wetting in liquid-solid system (Mullin, 2001).

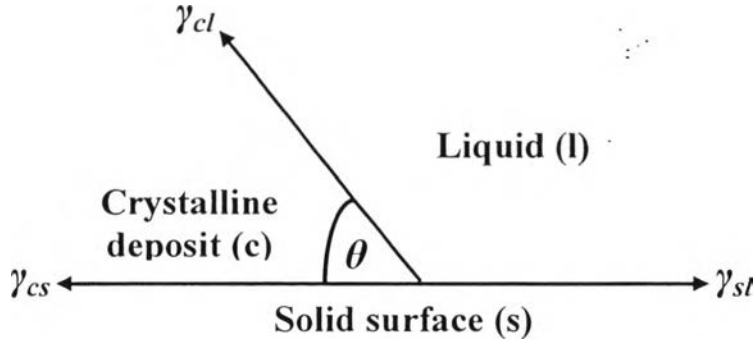

Figure 4.11 Interfacial tension at the boundaries between three phases (two solids, one liquid) (Mullin, 2001).

The factor ϕ in Equation (4.2) can be express as

$$\phi = \frac{(2+\cos\theta)(1-\cos\theta)^2}{4} \tag{4.5}$$

Thus, when θ=180°, cos θ = -1 and ϕ = 1, Equation (4.2) becomes

$$\Delta G'_{crit} = \Delta G_{crit} \tag{4.6}$$

When θ lines between 0 and 180°, ϕ < 1; therefore,

$$\Delta G'_{crit} < \Delta G_{crit} \tag{4.7}$$

When θ = 0, ϕ = 0, and

$$\Delta G'_{crit} = 0 \tag{4.8}$$

This is illustrated in Figure 4.12, which shows a foreign particle in a supersaturated solution (Mersmann, 2001).

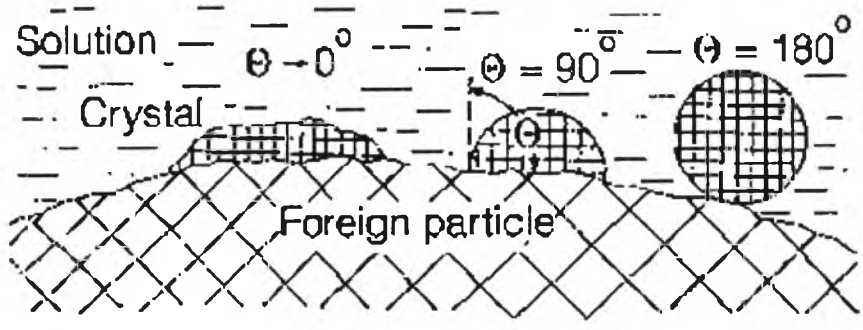

Figure 4.12 Nucleation on a foreign particle for different wetting angles (Mersmann, 2001).

For the cases of complete non-affinity between the crystalline solid and the foreign solid surface (corresponding to that of complete non-wetting in liquid-solid system), θ=180°, and Equation (4.6) applies, i.e. the overall free energy of nucleation is the same as that required for homogeneous or spontaneous nucleation. For the case partial affinity (cf. the partial wetting of a solid with a liquid), $0<\theta<180°$, and Equation (4.7) applies, which indicates that nucleation is easier to achieve because the overall excess free energy required is less than that for homogeneous nucleation. For the case of complete affinity (cf. complete wetting) θ=0, and the free energy of nucleation of zero. This case corresponds to the seeding of a supersaturation solution with crystals of the required crystalline product, i.e. no nuclei have to be formed in the solution (Mullin, 2001).

The presence of *m*- and *p*-CNB seeds may be in the case of the partial wetting of a solid with a liquid which is described by Equation (4.7), and ΔG_{crit} relate to $(\Delta T)^{-2}$ as indicated in Equation (4.9).

$$\Delta G_{crit} \alpha (\Delta T)^{-2} \quad (4.9)$$

where $\Delta T = T^* - T$ is the supercooling, T^* is the solid-liquid equilibrium temperature, and T is degree of supersaturation (Mullin, 2001).

From Equations (4.2), (4.7) and (4.9), the value of $\Delta G'_{crit}$ will be less than ΔG_{crit} when the value of ΔT is high that means the value of T or degree of supersaturation must be low. This relates to "The presence of a suitable foreign body or 'sympathic' surface can induce nucleation at degree of supercooling lower than those require for spontaneous nucleation (Mullin, 2001)." The metastable zone width may become broader. Thus, the crystallization temperature of the feed with the seeds decreases from the crystallization temperature of the feed without any seeds. The presence of the seeds may change the properties of the solution structure. The binary phase diagram of *m*- and *p*-CNB may be shifted to the right hand side. That is a reason why the precipitate composition in the feed at the eutectic composition is shifted from being rich in *m*-CNB to *p*-CNB (Mullin, 2001).

In addition, to investigate the effects of different seed sizes on precipitate composition, the *m*- and *p*-CNB seeds with different particle sizes, 20/40 and 12/14 mesh, were used. With the *m*-CNB seed, regardless of the size, the crystallization of the feed below the eutectic composition (61.0 wt% *m*-CNB) starts at 25 °C. However, the eutectic temperature of the feed with the 20/40 mesh *m*-CNB is 21.5 °C, which is slightly higher than that with 12/14 mesh *m*-CNB about 0.5 °C. The eutectic composition of the system with 20/40 or 12/14 mesh *m*-CNB is 65.0 wt%. By contrast, the eutectic temperature is changed to 19.0 °C and 19.5 °C when the seeds are 20/40 mesh and 12/14 mesh *p*-CNB, respectively, whereas the eutectic composition is the same as in the case of *m*-CNB seed. Again, for both 20/40 and 12/14 mesh of *m*- and *p*-CNB seeds, the precipitates below the eutectic compositions are rich in *p*-CNB and above the eutectic compositions are rich in *m*-CNB. It can be seen that the different seed sizes do not affect the crystallization temperature and the precipitate composition. From the result, a seed type only affects the crystallization temperatures, as seen in Figure 4.13.

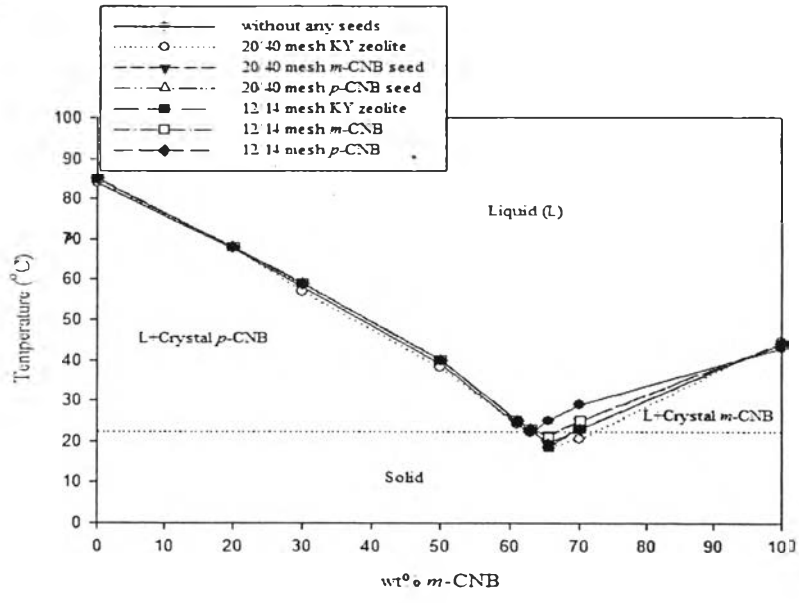

Figure 4.13 Binary phase diagram of *m*- and *p*-CNB with the presence of 20/40 and 12/14 mesh *m*-CNB seed, *p*-CNB seed, and KY zeolite size.

On the whole, the reason that the precipitates below the eutectic composition with the seeds (61.0 wt% *m*-CNB) can occur and grow at 25 °C can be explained by the general phenomenon of nucleation in the bulk and on the surface of seed crystals in batch crystallization processes, as shown in Figure 4.14.

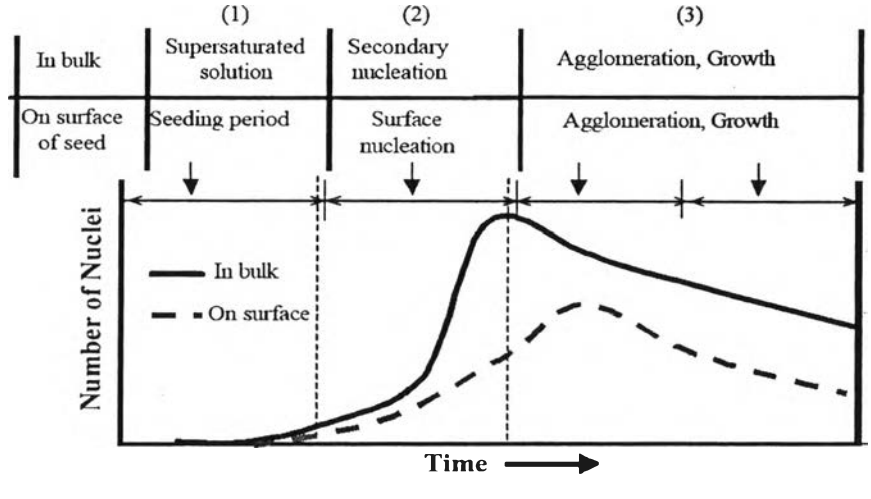

Figure 4.14 Typical phenomenon of nucleation in bulk and surface of seeds (Kim and Ulrich, 2003).

In the supersaturated solutions, there are three periods in relation to elapsed time: (1) seeding period, (2) surface nucleation period, and (3) growth period (agglomeration and crystal growth). Homogeneous/heterogeneous nuclei occur in the time period (1) within the metastable zone width (MZW). Secondary nucleation in the bulk can take place in time period (2) due to presence of the seeds. This means that the width of metastable zone becomes narrower. At the same time, surface nucleation takes place on the surface of the seed crystals. However, the number of surface nuclei is lower than those in the supersaturated bulk. After the secondary nucleation and surface nucleation, these nuclei start to agglomerate and grow in the time period (3) on the surface of seed particles simultaneously (Kim and Ulrich, 2003). With the presence of seed crystal at 25 °C, the precipitates can occur and grow at this temperature, which is higher than the crystallization temperature of that feed composition, because metastable zone is narrower.

Base on the phenomenon of nucleation in bulk and surface of seeds, if the number of nuclei in the primary nucleation is larger, the number of nuclei in the secondary nucleation will be larger leading to agglomeration. Agglomeration in the bulk can occur more than in the area of seeds because of higher number of nuclei, which, in turn, increases the chance in the nuclei collision. When two particles collide, they can entrain mother liquor during the agglomeration leading to a low product purity of precipitate composition.

Additionally, adding *p*-CNB seed causes the purity reduction of *m*-CNB precipitate composition when the crystallization starts from the feed above the eutectic compositions. As the number of seed crystals is larger and particle size is smaller, the purity decreases by agglomeration. Because of the increase of the number of elementary crystals constituting agglomerates, the purity of agglomerates decreases. The amount of mother liquor entrained during agglomeration becomes larger when the elementary crystals agglomerate more densely (Funakoshi *et al.*, 2001). As aforementioned, the *p*-CNB seed particles cause the lower purity of *m*-CNB precipitate compositions.